Understanding Local Defects in Li-ion Battery Electrodes through Combined DFT/NMR Studies: Application to $LiVPO_4F$

T. Bamine[a,b], E. Boivin[a,b,f], F. Boucher[c], R. J. Messinger[b,d,e], E. Salager[b,d], M. Deschamps[b,d],

C. Masquelier[b,f], L. Croguennec[a,b], M. Ménétrier[a,b] and D. Carlier[a,b*]

[a] *CNRS, Univ. Bordeaux, Bordeaux INP, ICMCB UPR 9048, F-33600 Pessac, France*

[b] *RS2E, Réseau Français sur le Stockage Electrochimique de l'Energie, FR CNRS 3459, F-80039 Amiens Cedex 1, France*

[c] *Institut des Matériaux Jean Rouxel (IMN), Université de Nantes, CNRS, 44322 Nantes, France*

[d] *CNRS, CEMHTI, UPR 3079, Université d'Orléans, Orléans, France*

[e] *Department of Chemical Engineering, The City College of New York, CUNY, New York, NY 10031 USA*

[f] *Laboratoire de Réactivité et de Chimie des Solides, CNRS-UMR#7314, Université de Picardie Jules Verne, F-80039 Amiens Cedex 1, France*

[*] Corresponding author (D. Carlier): dany.carlier@icmcb.cnrs.fr

Supporting Information

1- Validation of PAW method

Figure S1 shows the calculated shifts obtained for ^{7}Li in the olivine materials using the PAW and FP-LAPW methods and compared with the experimental ones. The olivine-type materials $LiMPO_4$ (M = Co, Ni, Mn, and Fe) exhibit all a single Li site. As discussed previously, no matter the method used, GGA or GGA+U with PAW or FP-LAPW approaches, the sign of the calculated shifts and the relative order of magnitude are well reproduced for all compounds.

For the Mn, Fe, and Co compounds a better agreement with the experimental shifts is obtained using GGA+U calculations for PAW and FP-LAPW methods, as expected by a stronger localization of the d electrons on the transition metal. Even if the calculated shifts are always larger that the experimental ones, the best agreement is clearly obtained for the FP-LAPW method (Wien2k code). For the Ni compounds however, calculations yield a fairly good agreement with the experimental shifts. As discussed in the text, this difference in behavior can result from the electronic configuration of LS-Ni^{2+} ions in octahedral sites (t_{2g}^6, e_g^2) that only exhibit two unpaired e_g electrons, whereas Mn^{3+} (t_{2g}^3, e_g^1), and Fe^{3+} (t_{2g}^3, e_g^2) do exhibit also unpaired t_{2g} electrons. These latter electronic configurations may strongly polarize deeper doubly occupied core levels that are better treated within the FP-LAPW than with the PAW approach.

Figure S1 shows the calculated shifts obtained for ^1H in the Tavorite materials with the PAW and FP-LAPW methods compared with the experimental ones. In this case, the two codes give a good agreement with the experimental results for ($LiFePO_4.OH$, $FePO_4.H_2O$, and $MnPO_4.H_2O$), but not for $LiMnPO_4.OH$ using PAW.

Figure S1 shows the calculated shifts obtained for ^{31}P in the Tavorite materials with the PAW and FP-LAPW methods compared with the experimental ones. The Tavorite-type materials except $LiVOPO_4$ exhibit all a single P site.

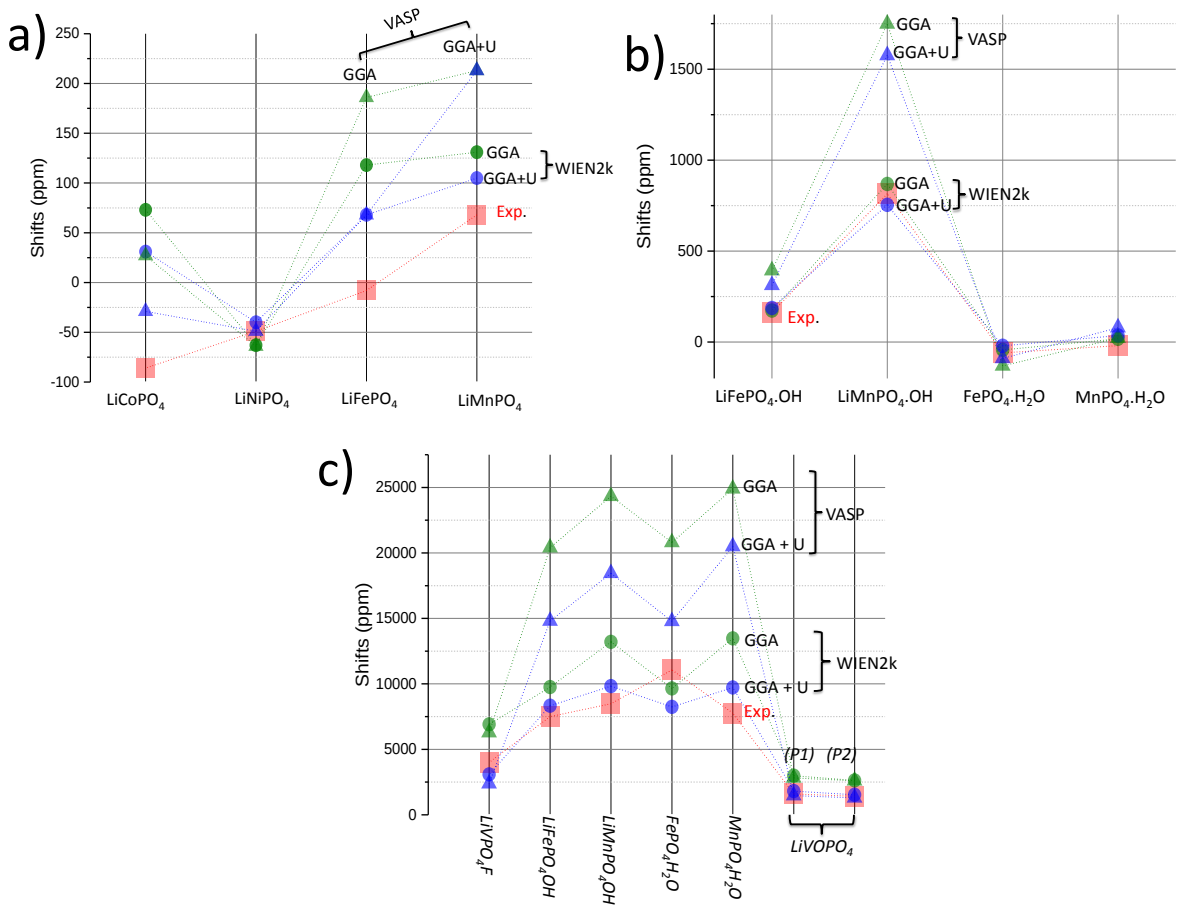

Figure S1: The calculated shifts obtained in the olivine materials using the PAW and FP-LAPW methods and compared with the experimental ones, a) for ^{7}Li, b) for ^{1}H, and c) for ^{31}P.

2- Geometry optimization

Table S2 gives relaxed cell parameters of $LiVPO_4F$, $LiVPO_4F_{0.94}O_{0.06}$, and $Li_{0.94}VPO_4F_{0.94}O_{0.06}$ obtained by the GGA and GGA+U methods with the VASP code as compared to the experimental cells. The cell parameters are slightly overestimated for all the materials. For all cases, the GGA+U calculation gives closer cell parameters than the GGA one.

		a (Å)	b (Å)	c(Å)	α (°)	β (°)	γ (°)
$LiVPO_4F$	Exp.	5.21	5.36	7.35	108.0	107.9	98.15
	GGA	5.17	5.30	7.26	107.5	107.9	98.38
	GGA+U	5.25	5.39	7.46	107.6	108.4	97.52
$LiVPO_4F_{0.94}O_{0.06}$	GGA	10.43	10.72	14.70	108.10	107.85	98.08
	GGA+U	10.48	10.80	14.89	108.55	108.18	97.26
$Li_{0.9}4VPO4F_{0.94}O_{0.06}$	GGA	10.43	10.70	14.72	108.21	107.89	97.95
	GGA+U	10.48	10.76	14.90	108.54	108.12	97.17

3- Bader charges

Table S3 shows partial charge calculated for the two V in $LiVPO_4F$, and the 16 vanadium in the supercell for both defect hypotheses, and clearly shows that V13 (V1') has the largest partial charge compared to other vanadium ions in the structure. Also, in $Li_{0.94}VPO_4F_{0.94}O_{0.06}$ the partial charges of V5 (V1') and V13 (V2') are equal and larger than for other V^{3+} in the structure.

V	***1***	***2***	***3***	***4***	***5***	***6***	***7***	***8***	***9***	***10***	***11***	***12***	***13***	***14***	***15***	***16***
$LiVPO_4F$	1.87	1.89	--	--	--	--	--	--	--	--	--	--	--	--	--	--
$LiVPO_4F_{0.94}O_{0.06}$	1.86	1.86	1.85	1.86	1.84	1.85	1.85	1.86	1.87	1.87	1.87	1.87	1.98	1.87	1.86	1.86
$Li_{0.94}VPO_4F_{0.94}O_{0.06}$	1.85	1.85	1.85	1.86	2.00	1.85	1.86	1.85	1.87	1.87	187	1.88	1.98	1.86	1.86	1.87

4- Magnetizations

Table S4 shows the magnetization in a 0.64 Å radius sphere around V (ionic radius size for a V^{3+} ions in [6] environment), it appears clearly that these two V ions are in the +IV state (S = ½) whereas the others remain +III (S = 1).

V	*1*	*2*	*3*	*4*	*5*	*6*	*7*	*8*	*9*	*10*	*11*	*12*	*13*	*14*	*15*	*16*
$LiVPO_4F$	1.97	1.92	--	--	--	--	--	--	--	--	--	--	--	--	--	--
$LiVPO_4F_{0.94}O_{0.06}$	2.00	2.00	2.00	1.97	2.00	2.00	2.00	1.99	1.99	1.98	1.99	1.98	1.19	1.98	2.00	1.99
$Li_{0.94}VPO_4F_{0.94}O_{0.06}$	2.00	2.00	2.00	2.00	1.14	2.00	2.00	2.00	1.98	1.98	1.98	1.98	1.18	1.98	2.00	1.99

5- ^{7}Li NMR of $LiVPO_4F$

In some samples, with different defect amount as reported in Ref. 13, we could better observe experimentally the splitting of the spectra at high shift around 187 ppm (186 ppm, and 182 ppm). **Figure S5** shows a zoom of this region.